Full Length Article

JHS(E)

Four-dimensional rotational radiographic scanning of the wrist in patients after proximal row carpectomy

The Journal of Hand Surgery
(European Volume)
2017, Vol. 42E(8) 846–851

DOI: 10.1177/1753193417718427
journals.sagepub.com/home/jhs

A. Peymani[1], M. Foumani[1], J. G. G. Dobbe[2], S. D. Strackee[1] and G. J. Streekstra[2]

Abstract

We measured cartilage thickness, contact surface area, volume of the capitate and shape of the capitate during motion in the operated and unaffected wrists of 11 patients with a mean follow-up of 7.3 years after proximal row carpectomy. Radiocapitate cartilage thickness in the operated wrists did not differ significantly from radiolunate cartilage thickness in the unaffected wrists. The radiolunate surface area was significantly less than the radiocapitate surface area. The volume of the capitate was significantly increased in the operated wrists. The shape of the capitate changed significantly in two of three orthogonal directions. The combination of remodelling of the capitate, increase in its surface area and intact cartilage thickness could help to explain the clinical success of proximal row carpectomy.

Keywords

Wrist, proximal row carpectomy, biomechanics, dynamic wrist imaging

Date received: 3rd February 2017; revised: 6th June 2017; accepted: 7th June 2017

Introduction

Proximal row carpectomy (PRC) is used in the treatment of various post-traumatic and degenerative disorders of the wrist (Inglis and Jones, 1977). In many patients, it provides good long-term results, including maintenance of function and pain relief (Berkhout et al., 2015; Richou et al., 2010).

The biomechanics of the wrist after PRC may provide information about the mechanisms whereby these results are attained. Until now they have been studied almost exclusively in static cadaveric models; this has several disadvantages, including the need to artificially load tendons and the disruption of ligaments (Blankenhorn et al., 2007; Hogan et al., 2004; Tang et al., 2009; Zhu et al., 2010). It is also not possible to investigate the changes that occur after soft tissue healing, scar tissue formation, capsular scarring and bone remodelling over time (Debottis et al., 2013; Tang et al., 2009; Zhu et al., 2010).

The purpose of our study was to investigate the effects of PRC on wrist joint kinematics in patients.

Methods

Setting and study population

A total of 64 individuals who had undergone a unilateral PRC between 1998 and 2007 were invited to take part in the study. Patients were invited if they had normal non-operated contralateral wrists without any history of trauma or systemic diseases. Eleven patients agreed to participate. The mean post-operative follow-up was 7.3 years (SD 3.4; range 1.9–10.7). The participants underwent computed tomography (CT) and four-dimensional rotational radiographic (4D-RX) scanning (Carelsen et al., 2005) of both wrists.

Additionally, to investigate any anatomical differences between the carpal bones of the left and right hand, 12 healthy participants (four men, eight women; mean age of 24, SD 2.4, range 22–31) were studied. These participants had no history of congenital wrist abnormalities or wrist injuries and underwent CT-scans of both wrists.

[1]Department of Plastic, Reconstructive and Hand Surgery, University of Amsterdam, Amsterdam, The Netherlands
[2]Department of Biomedical Engineering and Physics, University of Amsterdam, Amsterdam, The Netherlands

Corresponding author:
A. Peymani, Department of Plastic, Reconstructive and Hand Surgery, Academic Medical Center, University of Amsterdam, Room G4-226, Meibergdreef 9, PO Box 22660, 1100 DD Amsterdam, The Netherlands.
Email: a.peymani@amc.uva.nl

The local medical ethics committee approved this study.

Assessment and measurement of carpal bone kinematics

To record wrist bone positions during motion we used 4D-RX imaging (Carelsen et al., 2005). This method uses a static CT scan to obtain virtual three-dimensional (3D) models of the radius, ulna and carpal bones through segmentation (Figure 1) by the use of a previously described algorithm (Carelsen et al., 2009). Using a regular 3D rotational X-ray system (BV Pulsera, Philips Healthcare, The Netherlands), the static CT scans are combined with dynamic scans made during three motions: flexion-extension motion, radio-ulnar deviation and dart-throwing motion. Finally, virtual bone models are aligned with dynamic scans by registration, thereby quantifying motion patterns of wrist bones in vivo (Foumani et al., 2009, 2013).

A motorized hand-shaker device (Carelsen et al., 2009) was used to move the wrist with an imposed range of motion (ROM) set for each patient individually to avoid any pain or discomfort. During each of the three motions the X-ray source was rotated around the wrist to acquire 20 volume reconstructions, each reconstruction corresponding to a unique wrist position.

Assessment of 4D-RX imaging data in a previous study demonstrated a precision of 0.02 mm (SD 0.005) for translation and 0.12° (SD 0.07) for rotation (Carelsen et al., 2009).

Computation of joint space thickness and articular surface area

Individual articular cartilage layers could not be visualized owing to limitations of CT imaging; however, subchondral bone just below the cartilage layer was clearly definable. Total cartilage thickness could therefore be approximated by determining the distance between opposing subchondral bones. In this study, the joint space thickness was defined as the thickness of articular cartilage between the lunate and radius (unaffected wrists), or between the capitate and radius (operated wrists).

For each wrist position, joint space thickness was calculated using a previously specified method (Foumani et al., 2013). To this end, for each point on a bone, the nearest point to the opposite bone was determined using a k-Nearest Neighbors algorithm (Supplementary Video 1). To filter points contributing to the articular surface, two constraints were applied. First, the distance between a point on a bone and a point on an opposite bone should be less than 4 mm.

Figure 1. 3D reconstruction of the radius, ulna and carpal bones after segmentation.

The second constraint was a maximum angle difference of 15° between the normal vector of a point (vector perpendicular to the bone surface) and the normal vector of an opposite point. Thresholds of 4 mm and 15° were chosen pragmatically (Foumani et al., 2013). Joining all these points during motion provided the articular surface area defined as the area on the radius with which the lunate or capitate articulates (Figure 2).

The minimum distance to the opposite bone during motion was determined for each point, representing a situation where articular cartilage layers were minimal. The mean of these distances for all points in the articular surface area provided the joint space thickness. The mean joint space thickness was calculated by taking the mean of the radius-to-lunate and lunate-to-radius distances (unaffected wrists) or the mean of the radius-to-capitate and capitate-to-radius distances (operated wrists).

The joint space thickness and articular surface areas were recalculated for the combination of all three motions (60 wrist positions in all).

Assessment of the volume and shape of the capitate

The volume of the capitate was calculated from its virtual model. To enable shape comparisons, each

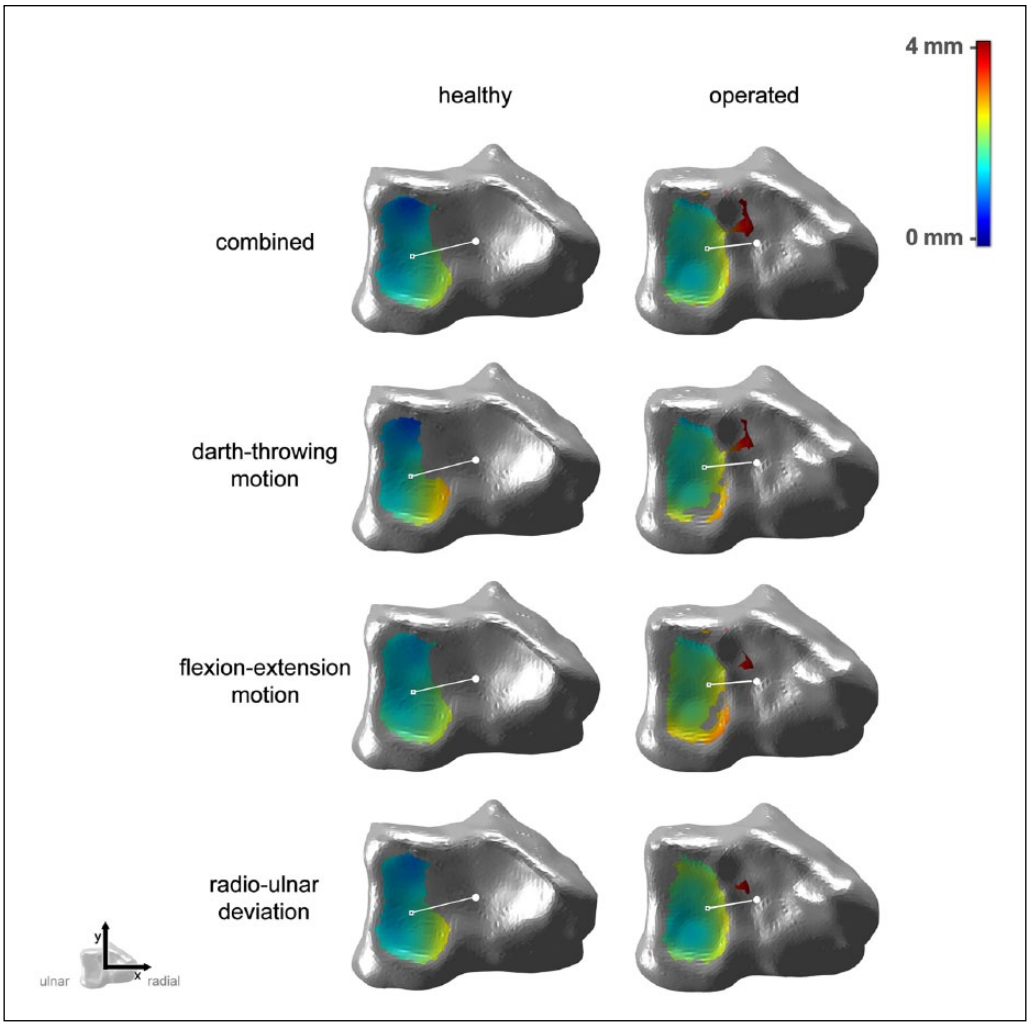

Figure 2. Articular surface areas of the radius with the lunate (left) and capitate (right). The colour map indicates the shortest distance to the neighbouring bone during the entire motion.

capitate was described as an ellipsoid with three gravitational axes (Goldstein et al., 2002) of lengths (ranked in order, from largest to smallest) *A, B* and *C* (Figure 3).

To determine whether any differences between capitates were due to naturally occurring anatomical differences, we repeated our assessment comparing healthy left and right wrists using CT imaging data from 12 healthy volunteers.

Statistical analysis

All variables followed a normal distribution, confirmed by Shapiro–Wilk tests. Paired samples *t*-tests were used to investigate the differences between unaffected wrists and operated wrists for joint space thickness, articular surface area, volume and shape parameters (lengths of ellipsoid axes) of the capitate.

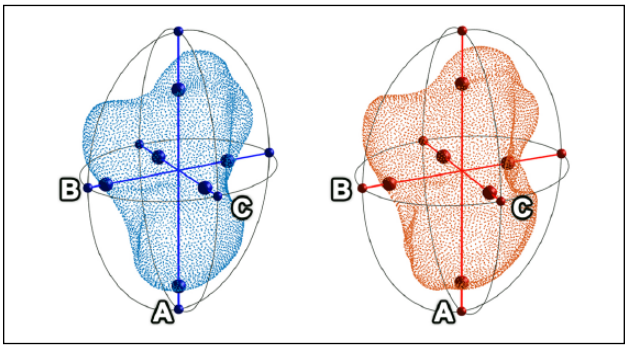

Figure 3. The capitate bone represented as an ellipsoid in the healthy (blue) and the operated wrist (red) with axes *A, B* and *C*.

Results

The characteristics of the 11 patients in the study are described in Table 1.

Table 1. Characteristics of the study group.

Variables	Proximal row carpectomy patients ($n = 11$)
Women	6
Mean age at surgery, years (SD; range)	43 (11; 19–59)
Mean age at follow-up, years (SD; range)	50 (10; 30–63)
Indication for surgery	
Kienböck's disease	4
SNAC	2
SLAC	1
Other	4
Mean imposed range of motion, degrees (SD; range)	
Unaffected wrist	
Dart-throwing motion	53 (10; 37–73)
Flexion-extension motion	79 (12; 55–93)
Radio-ulnar deviation	49 (10; 34–64)
Operated wrist	
Dart-throwing motion	43 (11; 23–60)
Flexion-extension motion	59 (15; 37–79)
Radio-ulnar deviation	33 (10; 19–44)

SNAC: scaphoid nonunion advanced collapse; SLAC: scapholunate advanced collapse.

Table 2. Joint space thickness and articular surface area.

Variables	Unaffected wrists ($n = 11$)	Operated wrists ($n = 11$)	p-value
Mean joint space thickness, mm (SD; range)			
Dart-throwing motion	1.5 (0.4; 0.8–2.2)	1.5 (0.6; 0.8–3.0)	0.797
Flexion-extension motion	1.4 (0.3; 1.0–1.9)	1.5 (0.5; 1.0–2.4)	0.864
Radio-ulnar deviation	1.4 (0.4; 0.8–1.9)	1.4 (0.4; 0.9–2.0)	0.982
Combined[a]	1.3 (0.3; 0.8–1.9)	1.3 (0.5; 0.7–2.4)	0.963
Mean articular surface area, cm^2 (SD; range)			
Dart-throwing motion	1.2 (0.3; 0.7–1.6)	1.3 (0.3; 0.8–2.0)	0.252
Flexion-extension motion	1.2 (0.3; 0.8–1.7)	1.5 (0.3; 1.0–2.0)	**0.029**
Radio-ulnar deviation	1.3 (0.3; 0.8–1.6)	1.2 (0.3; 0.8–1.9)	0.724
Combined[b]	1.4 (0.3; 0.9–1.8)	1.7 (0.4; 1.1–2.3)	**0.014**

[a]Joint space thickness (mm) combined for all three motions.
[b]Articular surface (cm^2) combined for all three motions.
Significant differences shown in bold.

The biomechanical comparison between operated and unaffected wrists is presented in Table 2. There were no significant differences in mean joint space thickness between operated and unaffected wrists. However, the articular surface area in operated wrists was significantly larger compared with unaffected wrists. When comparing the area of the articular surface for different motions, the difference was only significant for flexion-extension motion.

In Table 3 the differences in volume and shape of the capitate are shown. The volume of the capitate was significantly larger in operated wrists than in unaffected wrists. Shape comparisons displayed significantly longer *B* and *C* axes in the capitate after PRC. The volume and shape of the capitate did not differ significantly between the left and right wrists of 12 healthy volunteers.

Discussion

In this case-series study it was shown that after PRC the mean joint space thickness stays intact and the articular surface area slightly increases. The capitate undergoes anatomical changes after PRC, its volume and size increasing significantly.

A major strength of this study was that features were investigated in patients instead of cadavers, allowing the natural processes of soft tissue healing and capsule scarring to occur (Blankenhorn et al., 2007; Debottis et al., 2013). Another strength was

Table 3. Volume and shape of the capitate.

Variables	Proximal row carpectomy patients			Healthy volunteers		
	Unaffected wrists ($n = 11$)	Operated wrists ($n = 11$)	p-value	Left wrists ($n = 12$)	Right wrists ($n = 12$)	p-value
Mean volume, cm^3 (SD; range)	3.5 (0.8; 1.9–4.7)	3.7 (0.9; 2.1–5.0)	**0.010**	3.2 (0.9; 2.0–4.8)	3.2 (0.9; 2.0–4.8)	0.828
Mean axis length, mm (SD; range)						
Ellipsoid axis *A*	34.0 (3.0; 27.5–37.0)	34.1 (3.2; 27.2–37.5)	0.389	32.3 (3.2; 27.2–37.2)	32.2 (3.0; 27.5–36.9)	0.240
Ellipsoid axis *B*	23.8 (2.4; 19.3–28.0)	24.6 (2.5; 20.7–27.9)	**0.003**	23.9 (2.3; 20.6–27.4)	23.8 (2.2; 20.7–27.0)	0.721
Ellipsoid axis *C*	19.0 (1.5; 16.3–21.3)	19.7 (1.7; 16.9–22.5)	**0.005**	18.7 (1.7; 16.6–21.3)	18.7 (1.8; 16.3–21.6)	0.308

Significant differences shown in bold.

that we investigated the wrist joint parameters in 3D space and in a dynamic setup covering the entire ROM. In contrast, previous studies have measured radiocapitate space in static configurations using two-dimensional imaging (Croog and Stern, 2008; DiDonna et al., 2004; Wall et al., 2013), ignoring changes in orientation and the positions of carpal bones during movement (Carelsen et al., 2005). A limitation of this study was the potential for selection bias. Out of the 64 invited persons, 11 persons agreed to participate. It is possible that patients with good results from surgery might have been more likely to participate.

We compared the operated and unaffected wrists in individual patients. It might be suggested that the differences found are due to anatomical differences between the left and right wrists. However, previous research showed no significant differences between the wrists of healthy volunteers and the unaffected wrists of patients (Foumani et al., 2015). We showed that there were no significant anatomical differences in the size and shape of the capitate in each wrist in healthy volunteers, supporting our belief that the differences found in patients are indeed effects of the PRC procedure itself.

In this study, we were able to witness the biomechanical effects after PRC on the wrist joint. The cartilage-containing areas of the lunate fossa and capitate remain intact even though a new articular surface has been established. Previous cadaveric studies have investigated biomechanical changes in the radiocapitate joint using low-pressure-sensitive contact film (Hogan et al., 2004; Tang et al., 2009; Zhu et al., 2010). These studies showed a significant increase of contact pressure in the radiocapitate joint. These increased forces could possibly cause capitate remodelling as shown in our study. Two of these cadaveric studies reported a decrease in the contact area of the lunate fossa (Tang et al., 2009; Zhu et al., 2010). In contrast, we found an increased surface area after PRC, which is not surprising as we measured surface area after years of capitate remodelling under the influence of increased contact pressure. Taken together, increased radiocapitate forces could provide a credible explanation for the remodelling and increased surface area of the capitate that were seen several years after surgery, highlighting the adaptive capacity of the wrist after major anatomical changes.

The mean follow-up of 7.3 years gives a relatively limited insight into the long-term effects of anatomical changes in the wrist joint, especially since degenerative changes have been documented mainly in studies with a long-term follow-up (Ali et al., 2012; DiDonna et al., 2004; Lumsden et al., 2008). Furthermore, all measurements in this study were done at a single time point. It would be valuable to investigate the changes using repeated measurements over longer periods.

In conclusion, the combination of remodelling of the capitate, the corresponding increase in the articular surface area and the unaltered joint space thickness could help to explain the clinical success of PRC.

Acknowledgements The authors would like to express their deepest appreciation to Joy Vroemen for providing capitate bone imaging data of healthy volunteers and Carlijn M. Stekelenburg for her assistance in performing wrist imaging scans.

Declaration of Conflicting Interests The authors declared no potential conflicts of interest with respect to the research, authorship, and/or publication of this article.

Funding The authors received no financial support for the research, authorship, and/or publication of this article.

Ethical approval The local medical ethics committee approved this study.

References

Ali MH, Rizzo M, Shin AY, Moran SL. Long-term outcomes of proximal row carpectomy: a minimum of 15-year follow-up. Hand (NY). 2012, 7: 72–8.

Berkhout MJL, Bachour Y, Zheng KH, Mullender MG, Strackee SD, Ritt MJPF. Four-corner arthrodesis versus proximal row carpectomy: a retrospective study with a mean follow-up of 17 years. J Hand Surg Am. 2015, 40: 1349–54.

Blankenhorn BD, Pfaeffle HJ, Tang P, Robertson D, Imbriglia J, Goitz RJ. Carpal kinematics after proximal row carpectomy. J Hand Surg Am. 2007, 32: 37–46.

Carelsen B, Bakker NH, Strackee SD et al. 4D rotational X-ray imaging of wrist joint dynamic motion. Med Phys. 2005, 32: 2771–6.

Carelsen B, Jonges R, Strackee SD et al. Detection of in vivo dynamic 3-D motion patterns in the wrist joint. IEEE Trans Biomed Eng. 2009, 56: 1236–44.

Croog AS, Stern PJ. Proximal row carpectomy for advanced Kienbock's disease: average 10-year follow-up. J Hand Surg Am. 2008, 33: 1122–30.

Debottis DP, Werner FW, Sutton LG, Harley BJ. 4-corner arthrodesis and proximal row carpectomy: a biomechanical comparison of wrist motion and tendon forces. J Hand Surg Am. 2013, 38: 893–8.

DiDonna ML, Kiefhaber TR, Stern PJ. Proximal row carpectomy: study with a minimum of ten years of follow-up. J Bone Joint Surg Am. 2004, 86-A: 2359–65.

Foumani M, Strackee SD, Jonges R et al. In-vivo three-dimensional carpal bone kinematics during flexion-extension and radio-ulnar deviation of the wrist: dynamic motion versus stepwise static wrist positions. J Biomech. 2009, 42: 2664–71.

Foumani M, Strackee SD, van de Giessen M, Jonges R, Blankevoort L, Streekstra GJ. In-vivo dynamic and static three-dimensional joint space distance maps for assessment of cartilage thickness in the radiocarpal joint. Clin Biomech (Bristol, Avon). 2013, 28: 151–6.

Foumani M, Strackee SD, Stekelenburg CM, Blankevoort L, Streekstra GJ. Dynamic in vivo evaluation of radiocarpal contact after a 4-corner arthrodesis. J Hand Surg Am. 2015, 40: 759–66.

Goldstein H, Poole CP, Safko JL. *Classical mechanics*, 3rd Edn. San Francisco, Addison Wesley, 2002.

Hogan CJ, McKay PL, Degnan GG. Changes in radiocarpal loading characteristics after proximal row carpectomy. J Hand Surg Am. 2004, 29: 1109–13.

Inglis AE, Jones EC. Proximal-row carpectomy for diseases of the proximal row. J Bone Joint Surg Am. 1977, 59: 460–3.

Lumsden BC, Stone A, Engber WD. Treatment of advanced-stage Kienbock's disease with proximal row carpectomy: an average 15-year follow-up. J Hand Surg Am. 2008, 33: 493–502.

Richou J, Chuinard C, Moineau G, Hanouz N, Hu W, Le Nen D. Proximal row carpectomy: long-term results. Chir Main. 2010, 29: 10–5.

Tang P, Gauvin J, Muriuki M, Pfaeffle JH, Imbriglia JE, Goitz RJ. Comparison of the "contact biomechanics" of the intact and proximal row carpectomy wrist. J Hand Surg Am. 2009, 34: 660–70.

Wall LB, DiDonna ML, Kiefhaber TR, Stern PJ. Proximal row carpectomy: minimum 20-year follow-up. J Hand Surg Am. 2013, 38: 1498–504.

Zhu Y-L, Xu Y-Q, Ding J, Li J, Chen B, Ouyang Y-F. Biomechanics of the wrist after proximal row carpectomy in cadavers. J Hand Surg Eur. 2010, 35: 43–5.